

Evaluation of Leaf and Bark Extracts of *Acacia tortilis* as Corrosion Inhibitors for Mild Steel in Seawater: Experimental and Studies

Ismat H. Ali*, Abubakr M. Idris, Mohammed H. A. Suliman

Department of Chemistry, College of Science, King Khalid University, Abha, Saudi Arabia, P. O box 9004

*E-mail: ismathassanali@gmail.com

Received: 16 February 2019 / Accepted: 12 April 2019 / Published: 10 June 2019

Corrosion is a serious phenomenon affecting metals and alloys, which reduces the value and efficiency of metallic and alloyed products and shortens their lifetime. The aim of this study was to develop inexpensive and eco inhibitors extracted from abundant native plants in Asir region, Saudi Arabia. Phytochemical screening was carried out for the ethanolic extracts from leaves and barks. Polyphenols, phenolic compounds and flavonoids were found the major groups. Both potentiodynamic polarization curves and electrochemical impedance spectroscopy were used to investigate the efficiency of the inhibitors. The maximum achievable IE% were 87.6% and 72.9% for ATL and ATB, respectively. The potentiodynamic polarization (PDP) tests revealed that both extracts act as mixed type inhibitors. The results obtained from electrochemical impedance spectroscopy (EIS) measurements indicate an increase in polarization resistance confirming the inhibitive capacity of tested inhibitors. The adsorption of the inhibitors on the steel surface follow Langmuir adsorption isotherm model and involves competitive physio-sorption and chemi-sorption mechanisms. EIS technique was utilized to investigate the effect of temperature on corrosion inhibition at 298K – 328K temperature range. Results confirm that the inhibition efficiency (IE%) of all inhibitors decrease slightly as temperature increases. The thermodynamic parameters for both inhibitors were calculated.

Keywords: Corrosion, *Acacia tortilis*, leaves, barks, steel, sea water

1. INTRODUCTION

Corrosion of the metals and alloys has become one of the principal safety and economic concern all over the world. In many industrial applications, metals and their alloys likely undergo chemical or electrochemical reaction with the environment and severely corroded. Previous studies reveals that among all metals, mild steel has drawn a significant attention due to its high mechanical strength and exceptionally low cost [1-3]. Seawater is known to be an aggressive corrosive medium for

metals and alloys because of its high salts content [4]. Mild steel is widely used in a broad spectrum of industries and machineries especially in chemical processing, water desalination plants, marine applications, metal processing equipment and refining construction related works in petroleum production units [5].

Nowadays, among the several class of organic inhibitors, the compounds which have N, O, and S donor heteroatoms, electron donating functional group, conjugated π -electrons are considered effective corrosion inhibitors [6-10]. Organic inhibitor molecules can slow the corrosion rate by adsorbing on the metallic surface and thereby forming a protective layer, which can separate metals from the attack of the corrosive medium. Nonetheless, most of the developed corrosion inhibitors are costly and have environmental hazardous nature. In recent years, inhibitors from plants origin have drawn attention because they are efficient, biodegradable, inexpensive, eco-friendly and can be obtained using cheap and easy procedures [11-15].

Leaves extracts from Loquat, *biden pilosa* and *Xanthium strumarium* recorded inhibition efficiency (IE%) of 96, 88 and 95, respectively, for mild steel corrosion in acidic medium [16,17].

The root extract of *Valeriana wallichii* acts as mixed type inhibitor and recorded high efficiency as corrosion inhibitor for mild steel [18]. Extracts of both treated and untreated waste of date palm tree including fiber and leaflets recorded efficiency of 78–81% for carbon steel in the presence of gum Arabic solution [19]. *Pongamia Pinnata* was examined as a an eco-friendly corrosion Inhibitor for Mild Steel in 1N sulfuric acid medium, the efficiency of the extract was found to be 95% [20]. Many organic and natural inhibitors were reported to be efficient inhibitors in sea water [21-28].

Enormous research has been conducted on the evaluation plant extracts on steel corrosion. However, very few research have considered the effect of plant extracts on corrosion behavior of mild steel in seawater. Hence, the aim of this study was to investigate the efficiency of leaf and bark extracts of *Acacia tortilis* as corrosion inhibitors for mild steel in seawater.

2. EXPERIMENTAL

2.1. Plant sample collection

Leaves and barks of *A. tortilis* abbreviated as ATL and ATB, respectively, were collected in April/May 2017 from some areas around Khamees-Mushait city, Asir Region, Saudi Arabia. Barks and leaves were rinsed thoroughly with tap water to get rid of soil particles followed by bi-distilled water. The barks were cut into small pieces and air-dried under shade at room temperature for two weeks. Samples were later ground to fine powder to give 400 g of barks and 200 g of leaves.

2.2. Extraction of plant samples

Each sample was macerated in aqueous ethanol (ethanol: water, 80% v/v) at room temperature for 3 to 5 days with occasionally stirring. Extract was collected after each 36 h by decantation and fresh solvent was added to the residue. Collected extracts were filtered through Whatman No 1 filter paper, combined and concentrated to dryness under reduced pressure at 40°C using a rotary evaporator

(IKA R10, C S99-China). The obtained concentrated extracts were weighed and stored in a refrigerator (- 4°C), until used for analyses.

2.3. Scanning and verification of extract

2.3.1. Phytochemical Screening of the Crude Extracts:

The ethanolic extracts were subjected to preliminary phytochemical screening for different phytoconstituents (alkaloids, saponins, glycosides, flavonoids, tannins, triterpenes, anthraquinones and phenolic compounds) by adopting standard protocols [29].

2.3.2. Determination of Total Phenolic and Flavonoid Contents:

The total phenolic content (TPC) in the extracts were estimated colorimetrically using the Folin-Ciocalteu method with slight modification [30,31]. An aliquot of 0.5 mL of each plant extract (1mg/mL) was mixed with 2.5 ml of 0.2N Folin-Ciocalteu reagent (Sigma–Aldrich) for 5 min. 2.0 mL of 7.5% sodium carbonate solution were then added. The mixture was allowed to stand for 2 h at room temperature for color development. The absorbance was then measured at 760 nm using UV-VIS spectrophotometer (JASCO UV/VIS Spectrophotometer, V-530, No. B184160512- Japan). Gallic acid standards were used to produce the calibration curve which was analyzed in the same way as the plant extract and total phenolic was expressed as Gallic acid equivalents (mg GAE /g of plant extract).

The total flavonoid content (TFC) of the extracts was measured as previously described[32], with modifications. 2 ml of 2% AlCl₃ methanol solution were added to 2 ml of plant extract. The mixture was stand for one hour at room temperature. The absorbance was measured at 415 nm using UV-VIS spectrophotometer. A yellow color indicated the presence of flavonoids. Quercetin was used for calibration. TFC was estimated as milligrams quercetin equivalents per gram of plant extract.

2.4. Steel samples

Most of the equipment of the desalination plant are made of mild steel, the composition of this alloys is: (0.189% C, 0.175% Si, 0.572% Mn, 0.197% Cu, 0.058% S and Fe balance. The dimensions of samples which used throughout all tests are 2.0 × 2.0 × 0.08 cm.

2.5. Corrosion measurements

2.5.1. Mass loss measurements

Before each test, the surfaces of all samples were abraded using emery papers of 1200, 800, 320 and 180 grades, then rinsed thoroughly with bi-distilled water, degreased and dried with acetone. Mass loss measurements were performed at 298K for 6, 12, 18 and 24 h.

2.5.2. Electrochemical tests

The electrochemical experiments were performed by using a potentiostat Gamry interface 1000 No. 06094 USA directed by Framework 7.07 software. A cell with three electrodes was connected with the thermostat. A Pt electrode and saturated calomel electrode were used as auxiliary and reference electrodes, respectively. The same material was used for both gravimetric and electrochemical experiments. Potentiodynamic polarization (PDP) tests were performed at a scan rate of 1.0 mV/s. The polarization curves were attained from -1000 mV to 1000 mV.

Measurements of electrochemical impedance spectroscopy (EIS) were accomplished using the same instrument (Gamry interface 1000). Prior to sine wave voltage (10 mV) peak to peak, at frequencies between 10^4 Hz and 10^{-3} Hz are superimposed on the rest potential, the steady-state current at a corrosion potential was determined. Computer programs automatically controlled the measurements performed at rest potentials after 1 hour of contact at 298 K. The EIS diagrams are obtained as Nyquist plots. To investigate the effects of temperature on inhibitors effectiveness, some experiments were performed at 298–328 K temperature range. To confirm reproducibility, all test were performed three times.

3. RESULTS AND DISCUSSION

3.1. Phytochemical Screening of the Crude Extracts

The phytochemical screening of ATL and ATB revealed positive tests of phenolics, flavonoids, glycosides, tannins, steroids and Saponins and negative tests of alkaloids and anthraquinones.

3.2. Determination of Total Phenolic and Flavonoid Contents:

Polyphenols, including phenolic compounds and flavonoids, constitute main groups of compounds acting as primary antioxidants or free radical scavengers. Their antioxidant activity is based on their ability to donate hydrogen atoms to free radicals and their stability as radical intermediates. These redox properties can play an important role in absorbing and neutralizing free radicals, quenching singlet and triplet oxygen or decomposing peroxides [33].

Total phenolic contents are quantified as Gallic acid equivalents by reference to regression equation ($y = 11.861x + 0.0001$, $R^2 = 0.9929$). Values of total phenols are expressed as means \pm standard deviation for three replicate measurements. The total phenolic contents of ATL and ATB are 125.90 ± 0.25 mg 287.03 ± 0.06 GAE/g, respectively.

Flavonoid content was calculated from the regression equation of the standard curve ($y = 28.9055x + 0.1608$, $R^2 = 0.9966$) and expressed as mg quercetin equivalents (QE) per gram of dried plant extract. The leaf extract of *A. tortilis* has high flavonoid content (77.03 ± 0.12), while the barks of *A. tortilis* contains only 3.30 ± 0.00 mg QE/g.

3.3. Mass loss measurements

The influence of adding several concentrations of ATL and ATB to the corrosive medium were examined by using mass loss method at 298 K.

The loss in the weight of steel pieces in uninhibited and inhibited seawater was determined. Equation 1 was used to determine the corrosion rate in millimeters per year (mm y^{-1}):

$$C_{RM} = \frac{K \times W}{A \times t \times \rho} \quad (1)$$

where $K = 8.76 \times 10^4$ was used as constant. W and t are the mass loss in grams and the exposure time in hours. According to ASTM G1-03 standard [34], the density of steel is 7.86 g cm^{-3} . The exposed area, A (in cm^2) was calculated from Equation 2 [35]:

$$A = \frac{\pi}{2} (D^2 - d^2) + l\pi D + l\pi d \quad (2)$$

where D , d and l are the diameter of mild steel pieces, the diameter of the hole for holding and the thickness, respectively. Equations 3 and 4 were used to calculate the inhibition efficiency inhibitor efficiency $IE_{ML} \%$ and the surface coverage (θ):

$$\eta_{WL} (\%) = \left[\frac{C_{RW}^{\circ} - C_{RW}}{C_{RW}^{\circ}} \right] \times 100 \quad (3)$$

$$\theta = \left[\frac{C_{RW}^{\circ} - C_{RW}}{C_{RW}^{\circ}} \right] \quad (4)$$

Where C_{RW}° and C_{RW} are the corrosion rates without and with various concentrations of the inhibitors, respectively, θ is the degree of surface coverage of tested inhibitors. Table 1 summarizes the obtained results. The inhibition efficiency and the corrosion rates of the steel in presence of inhibitors were found to increase continuously with an increase in their concentration. The order of the inhibition efficiencies at the same concentration is $ATL > ATB$. The results support the hypothesis states that by increasing the concentration of inhibitors, the adsorption of inhibitors will be gradually increased, leading to a complete blockage of corrosion of active sites except $1 - \theta$ of exposed surface area.

Table 1. Weight loss data of steel samples in uninhibited and inhibited seawater at 298K.

Inhibitors	C (g/L)	C_{RW} ($\text{mg. cm}^{-2} \cdot \text{h}^{-1}$)	$\eta_{WL} \%$	Θ
Blank	-	1.124	-	-
ATL	0.25	0.408	63.6	0.636
	0.50	0.321	71.4	0.714
	1.00	0.207	81.5	0.815
	1.50	0.126	88.7	0.887
ATB	0.25	0.557	50.4	0.504
	0.50	0.465	58.6	0.586
	1.00	0.400	64.4	0.644
	1.50	0.334	70.2	0.702

3.4. Stability of the inhibitors

To assess the stability of the inhibitive layer of the inhibitors under study and to conclude the time needed for the inhibitors to reach the maximum IE%, weight loss tests were accomplished in seawater with the optimum concentration of the inhibitors for various immersion times. The results are displayed in Figure 1. It obvious that IE% decreases as immersion time increases. The highest effectiveness was recorded at 1–6 h of immersion. When the immersion time was increased to 24 hours, a clear decrease in effectiveness was noticed. These results may be due to the instability of the inhibitor layer or due to the biodegradable nature of the plants extracts after a long time contact [36,37].

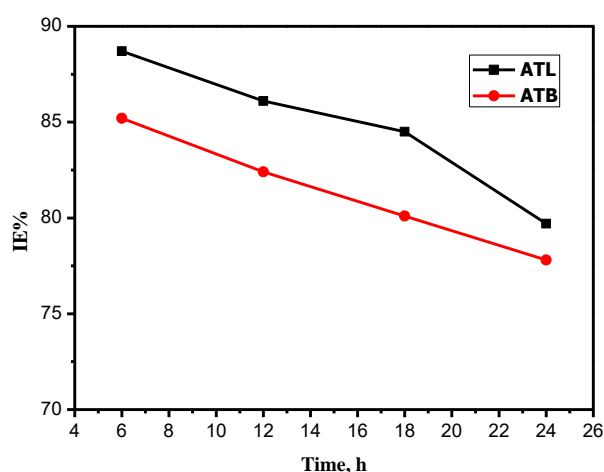


Figure 1. Effect of immersion time on the inhibition efficiency, for mild steel in sea water at 298K.

3.5. Electrochemical measurements

3.5.1. Potentiodynamic polarization curves

Figure 2 shows the Tafel polarization plots of different concentrations of ATL and ATB, respectively. The kinetic factors viz. corrosion current density (I_{corr}), anodic Tafel slopes, cathodic Tafel slopes (b_c) and corrosion potential (E_{corr}) were attained from these plots and are given in Table 2. Values of EI% were determined using Equation 5:

$$EI\% = \frac{I_{corr}^0 - I_{corr}}{I_{corr}^0} \times 100 \quad (5)$$

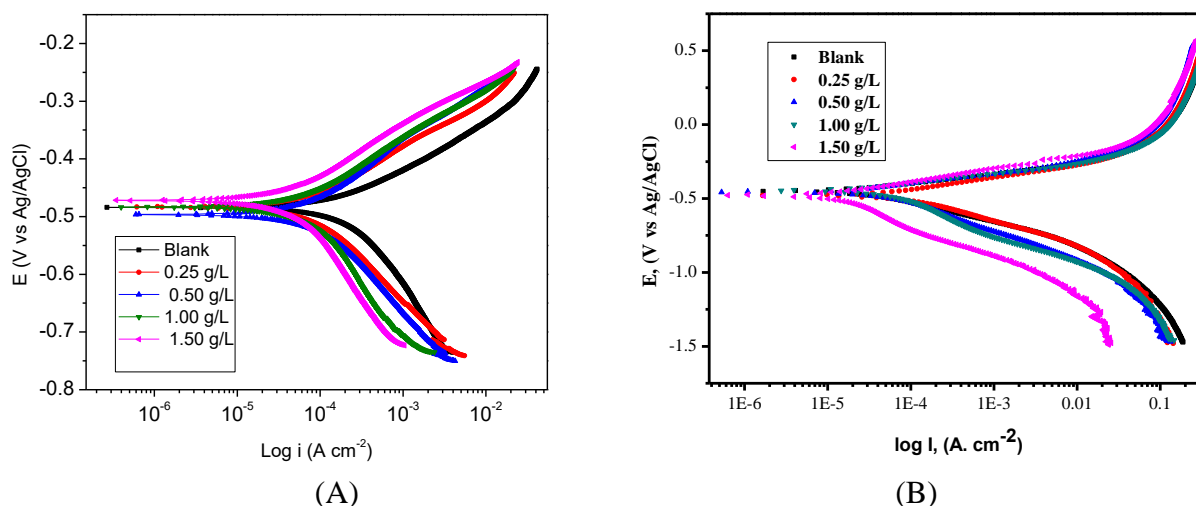
where I_{corr}^0 and I_{corr} are corrosion current densities of the steel samples without and with the inhibitors, respectively.

Results in Table 2 designate that, values I_{corr} decreased gradually with the increase of the inhibitors concentration. It is obvious that, values of the anodic Tafel slopes b_a and cathodic Tafel slopes, b_c differ slightly except at the lowest concentration indicating that mechanism of the proton discharge reaction does not change by addition of the inhibitors.

Table 2. Electrochemical parameters of steel at various concentrations of ATL and ATB in sea water and corresponding inhibition efficiency.

Inhibitor	Conc. (g/L)	$-E_{\text{corr}}$ (mV/SCE)	I_{corr} ($\mu\text{A cm}^{-2}$)	b_a (mV dec^{-1})	$-b_c$ (mV dec^{-1})	$\text{IE}_{I_{\text{corr}}}$ (%)
Blank	-	467	1437	157	227	----
ATL	0.25	477	577	172	217	59.8
	0.50	504	429	183	183	70.1
	1.00	514	263	166	191	81.7
	1.50	547	178	177	197	87.6
ATB	0.25	488	722	174	178	49.8
	0.50	497	609	162	185	57.6
	1.00	503	522	188	194	63.7
	1.50	485	435	176	181	69.7

Figure 2 reveals that all inhibitors suppressed both anodic and cathodic currents confirming mixed type inhibitor. IE% increases as the inhibitor concentration increases reaching a maximum values 87.6% and 69.7% for ATL and ATB, respectively.

**Figure 2.** Potentiodynamic polarization curves of steel in sea water in the presence of different concentrations of (A) ATL (B) ATB

3.5.2. Electrochemical impedance spectroscopy (EIS)

The EIS experiments were performed in uninhibited and inhibited seawater to obtain more information about the corrosion inhibition mechanism of the mild steel. EIS results are showed as Nyquist plots in Figure 3. The semicircles of EIS experiments were slightly depressed compared to those derived from the theory of EIS. The imperfectness of capacitive loop is a common behavior and it is attributed to the result of the heterogeneity, frequency dispersion and roughness of the steel

surface [38,39]. Curves have been obtained after 60 minutes of soaking the electrodes in the required concentration (open circuit potential).

It is clear from Figure 3 that single capacitive loops have been obtained for all inhibitors indicating that the mild steel dissolution at metal/seawater interface is controlled by charge transfer process. The inhibition efficiencies, EI_{R_t} (%) are displayed in Table 3.

Table 3. Electrochemical Impedance parameters for corrosion of the steel sample at various concentrations of the inhibitors at 298K

inhibitor	Concentration (g/L)	R_t ($\Omega \cdot \text{cm}^2$)	$Q \times 10^{-4}$ ($\text{S}^n \Omega^{-1} \text{cm}^{-1}$)	$(10^4) C_{dl}$ ($\mu\text{F}/\text{cm}^2$)	EI_{R_t} (%)
Blank	---	13	2.65	145.5	----
ATL	0.25	32	2.31	58.7	59.3
	0.50	35	1.97	36.9	62.9
	1.00	66	1.72	22.4	80.3
	1.50	104	1.61	6.9	87.5
ATB	0.25	27	2.57	64.4	51.8
	0.50	30	2.34	45.8	56.6
	1.00	39	2.18	31.6	66.6
	1.50	48	1.99	11.2	72.9

In order to determine R_t values, the high frequency impedance was subtracted from the low frequency one as shown in Equation 6:

$$R_t = Z_{re} \text{ (at low frequency)} - Z_{re} \text{ (at high frequency)} \quad (6)$$

C_{dl} values (electrochemical double layer) were determined at the frequency f_{max} , when the imaginary component of the impedance has a maximum value ($-Z_{max}$) by Equation 7:

$$C_{dl} = \frac{1}{2\pi f_{max} R_t} \quad (7)$$

The inhibition efficiency $IE\%_{(EIS)}$ is determined by using Equation 8:

$$EI\%_{(EIS)} = \frac{R_t^0 - R_t}{R_t^0} \times 100 \quad (8)$$

where R_t^0 and R_t are the charge transfer resistance values without and with the presence of the inhibitor, respectively.

It is understandable from Table 3 that the resistance values increase in the presence of all inhibitors. This can be ascribed to the effect of corrosion protection of the molecules. It is also can be noticed that C_{dl} values decrease in the presence of the inhibitor. This may be attributed to the local dielectric constant decrease and/or to the rise in the depth of the electric double layer [40,41], indicating that inhibitor molecules working by adsorption at the interface of the seawater/metal.

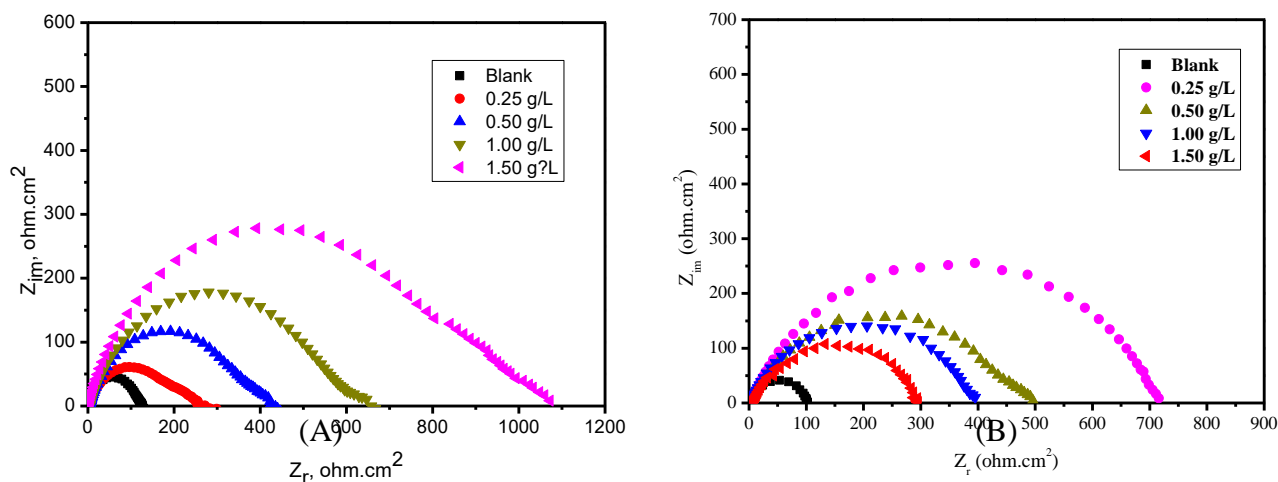


Figure 3. Nyquist diagrams for carbon steel electrode with and without (A) ATL and (B) ATB after 60 minutes of OCP.

The decrease of C_{dl} values and the increase of R_t values and hence, the IE% increase is likely due to the regular substitution of water molecules by the adsorbed inhibitors molecules on the steel surface, reducing the degree of iron oxidation [42,43]. The results concluded from EIS tests are in good agreement with those obtained from polarization tests.

3.6. Adsorption study

Adsorption study aims to discover the way by which the inhibitor molecules interact with the steel surface. Values of surface coverage, θ , at various inhibitor concentrations at 298K (Table 1) were employed to determine the adsorption isotherm. θ values were calculated by using Equation 9:

$$\theta = \frac{W_{corr}^o - W_{corr}}{W_{corr}^o} \tag{9}$$

There are many models of adsorption isotherms such as, Freundlich, D-R, Temkin and Langmuir isotherms.

Application of Equation 10 gives straight lines with slope values of 1.033, and 1.068 for ATL and ATB respectively. Also, good correlation coefficient ($R^2 > 0.997$) was obtained proving that the adsorption of the inhibitor molecules from seawater on the steel surface follows the Langmuir model.

$$\frac{C_{inh}}{\theta} = \frac{1}{K_{ads}} + C_{inh} \tag{10}$$

with

$$\Delta G_{ads} = -RT \ln (K_{ads} \times 999) \tag{11}$$

Values of equilibrium adsorption constant (K_{ads}) were determined from the intercept of Equation 10 and ΔG_{ads} values were calculated from Equation 11. Results are shown in Table 4.

Table 4. Values of K_{ads} and ΔG_{ads} for the adsorption process of ATL and ATB on mild steel at 298K.

Inhibitor	K_{ads}	ΔG_{ads} (kJ/mol)
ATL	6.13	-21.6
ATB	5.28	-21.4

Results in Table 4 indicate that values of adsorption free energy are negative, which suggests that the adsorption process is spontaneous. According to results reported previously, it is probably when the value of $\Delta G_{ads} \sim -40$ kJ/mol or more negative, the process is considered to be chemisorption, whereas if $\Delta G_{ads} \sim -20$ kJ/mol or less negative, the process is likely counted to be physio-sorption. In this study, the results designate the occurrence of both physical and chemical interactions [44-46].

3.7. Effect of temperature

(EIS) technique was adapted to explore the effect of temperature on the inhibition process and to obtain some thermodynamic parameters of the corrosion process. EIS experiments were performed at temperature range of 298-328 K without and with the optimal concentration of the inhibitors (Figure 4).

Table 5. Effect of temperature on the adsorption of various inhibitors (1.50 g/L) in sea water on the carbon steel at different temperatures.

Inhibitor	T (K)	R_t ($\Omega \cdot \text{cm}^2$)	$Q \times 10^{-4}$ $\text{S}^n \Omega^{-1} \text{cm}^{-1}$	C_{dl} ($\mu\text{F}/\text{cm}^2$)	EI_{R_t} (%)
Blank	298	13	2.65	145.5	---
	308	9	2.86	117	---
	318	7	2.98	130	---
	328	5	3.23	87	---
ATL	298	102	1.61	25	87.3
	308	51	1.82	41	80.7
	318	33	1.99	54	78.8
	328	19	2.25	71	73.7
ATB	298	48	1.99	31	72.9
	308	28	2.24	49	67.9
	318	17	2.47	62	58.8
	328	11	2.71	88	54.5

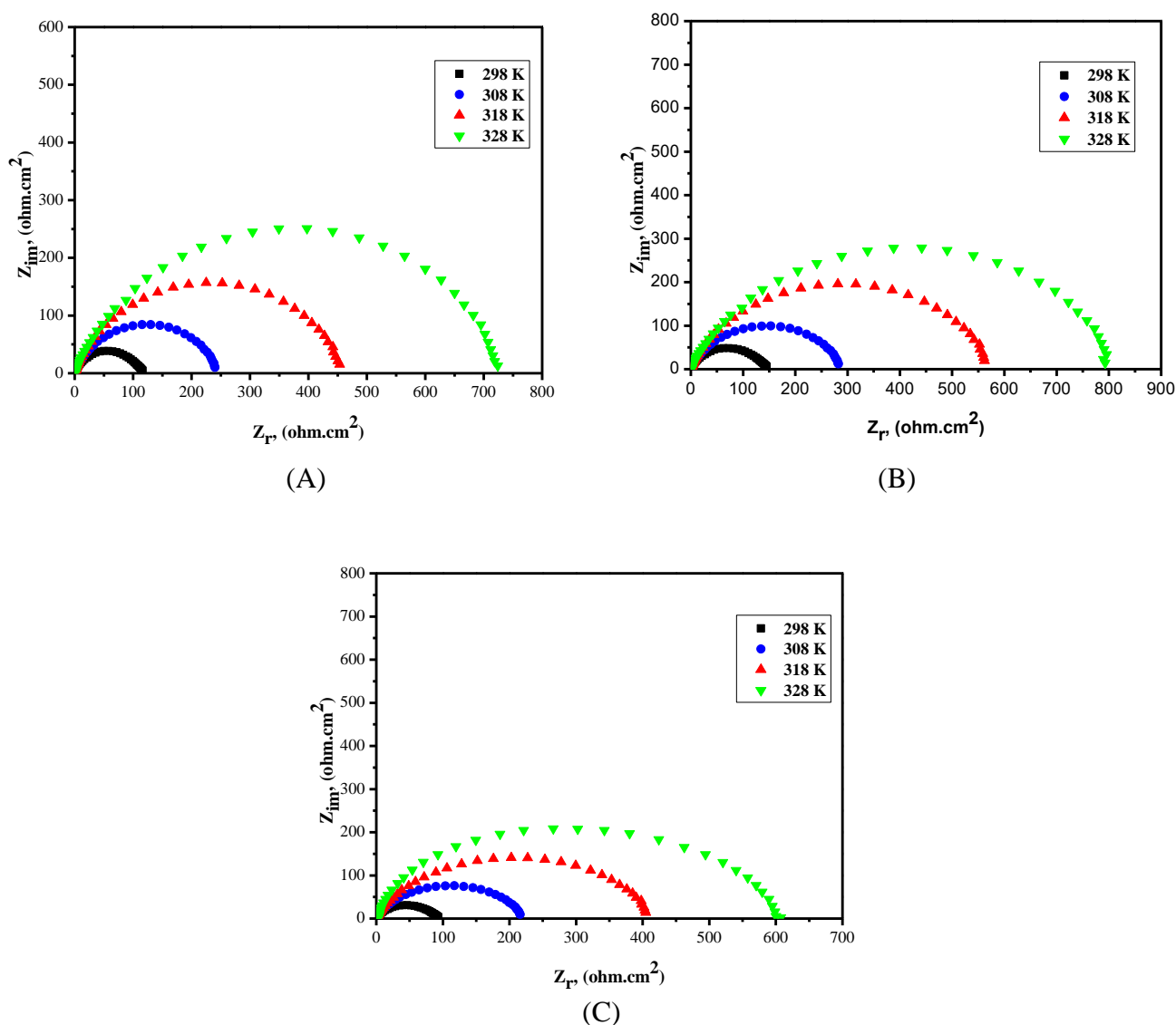


Figure 4. Nyquist diagrams for mild steel in sea water at different temperatures for (A) ATL (B) ATB (C) Blank

Results displayed in Table 5, confirm that the values of charge transfer resistance (R_t) decrease as the temperature increases in both inhibited and uninhibited media. Table 5 also reveals that IE% values in the presence of all inhibitors slightly decreased as the temperature increased. This is likely because the desorption process may take place at elevated temperatures. These results prove that ATL is an efficient inhibitor over the studied temperature range. It is clear that ATB efficiency is temperature dependent because its IE% decreased to only 54% at 328 K. This is a common behavior of inhibitors from plant origin [47,48].

The charge transfer resistance (R_t), was employed to calculate values of activation energy as shown in Arrhenius Equation (Equation 12). The entropy change (ΔS) and enthalpy change (ΔH) were obtained from the intercept and slope of Eyring equation (Equation 13).

$$\ln R_t = \ln A - \frac{E_a}{RT} \tag{12}$$

$$\ln \frac{R_t}{T} = \frac{-\Delta H}{RT} + \ln \frac{k_B}{h} + \frac{\Delta S}{R} \quad (13)$$

where E_a is the activation energy of the corrosion process, k_B is the Boltzmann constant, T is the absolute temperature, A is the frequency factor, h is Planck's constant. Values of ΔS , ΔH and E_a with and without 1.5 g/L of all inhibitors are shown in Table 6.

Table 6. The value of activation parameters for mild steel in sea water in the absence and presence of 1.50 g/L of inhibitors

Inhibitor	E_a (kJ/mol)	ΔH (kJ/mol)	ΔS (J/mol)
Blank	25.3	27.9	317.2
ATL	44.6	47.2	364.6
ATB	40.1	42.6	353.8

It is clear that the values of activation energy E_a , of the corrosion process, in the absence of all inhibitors, are smaller than that in the presence of them confirming that the corrosion process becomes more difficult after adding the inhibitors [49]. The order of increase of E_a is blank < ATB < ATL, which is in good agreement with the order of increase in the inhibition efficiency, It is also clear that the thermodynamic parameters (ΔS and ΔH) in the existence of the inhibitors are larger than those calculated in the absence of all inhibitor. The more positive sign of ΔH in the presence of the inhibitors indicates an endothermic nature of the corrosion process suggesting that the ionization of mild steel is slow in the presence of the inhibitors [50]. Large and positive values of entropy (ΔS) denote that during the rate determining step, the activated complex is formed via an association rather than a dissociation step [51], proving that an increase in disordering takes place on going from reactants to the activated complex [52].

4. CONCLUSION

ATL and ATB were used as corrosion inhibitors for mild steel sea water. The study was performed using various techniques which contain weight loss, electrochemical measurements. ATL displays a good inhibition efficiency, while ATB show a moderate to weak inhibition performance. The study reveals that both ATL and ATB suppress both the anodic and cathodic process (mixed-typed inhibitor) following Langmuir adsorption model. Results showed that the performance of both inhibitors decrease with time.

ACKNOWLEDGEMENTS

This research project was fully supported by the grant from King Abdulaziz City for Science and Technology (KACST), award number SP-37-84.

References

1. H. Ashassi-Sorkhabi, B. Shaabani and D. Seifzadeh, *Applied Surface Science*, 239 (2005) 154.
2. M. Bouanis, M. Tourabi, A. Nyassi, A. Zarrouk, C. Jama and F. Bentiss, *Applied Surface Science*, 389 (2016) 952.

3. K. Zhang, W. Yang, X. Yin, Y. Chen and Y. Liu, *Carbohydrate polymers*, 181 (2018) 191.
4. T. Peev, M. Georgieva, S. Nagy, A. Vertes, *Radiochemical and Radioanalytical Letters*, 33 (1987) 265.
5. N. Pessall and J. Nurminen, *Corrosion*, 30 (1974) 381.
6. H. Lgaz, K. S. Bhat, R. Salghi, S. Jodeh, M. Algarra, B. Hammouti, I. H. Ali and A. Essamri, *J. Mol. Liq.*, 238 (2017) 71.
7. H. Lgaz, R. Salghi and I. H. Ali, *Int. J. Electrochem. Sci.*, 13 (2108) 250.
8. H. Lgaz, R. Salghi, S. Jodeh and B. Hammouti, *J. Mol. Liq.*, 225 (2017) 271.
9. H. Lgaz, I. Chung, R. Salghi, I. H. Ali, A. Chaouiki, Y. El Aoufir, M. I. Khan, *Applied Surface Science*, 463 (2019) 647.
10. I. H. Ali, R. Marzouki, Y. B. Smida, A. Brahmia, M. F. Zid, *Int. J. Electrochem. Sci.*, 13 (2018) 11580.
11. I. H. Ali, *Int. J. Electrochem. Sci.*, 10 (2016) 2130.
12. L. Bammou, R. Salghi, A. Zarrouk, H. Zarrok, S. S. Al-Deyab, B. Hammouti, M. Zougagh and M. Errami, *Int. J. Electrochem. Sci.*, 7 (2012) 897.
13. A. Ennouri, A. Lamiri and M. Essahli, *Portugaliae Electrochimica Acta*, 35 (2017) 279.
14. Y. Sharma and S. Sharma, *Portugaliae Electrochimica Acta*, 34 (2016) 365.
15. F. Wedian, M. A. Al-Qudah and A. N. Abu-Baker, *Portugaliae Electrochimica Acta*, 34 (2016) 39.
16. X. Zheng, M. Gong, Q. Li and L. Guo, *Scientific reports*, 8 (2018) 9140.
17. S. Olusegun, T. Joshua, M. Bodunrin and S. Aribo, *Nature and Science*, 16 (2018) 1.
18. R. Haldhar, D. Prasad, A. Saxena and P. Singh, *Materials Chemistry Frontiers*, 2 (2018) 1225.
19. G. M. Al-Senani and M. Alshabanat, *Int. J. Electrochem. Sci.*, 13 (2018) 3777.
20. T. Bhuvaneshwari, V. Vasantha and C. Jeyaprabha, *Silicon*, (2018) 1.
21. A. El-Etre and M. Abdallah, *Corros. Sci.*, 42 (2000) 731.
22. V. Gouda, *British Corrosion Journal*, 5 (1970) 198.
23. E. Mor and C. Wrubl, *British Corrosion Journal*, 11 (1976) 199.
24. R. Shalon and M. Rapheal, Influence of sea water on corrosion of reinforcement. *Proc. Journal Proceedings*, 55 (1959) 1251.
25. E-SM. Sherif, R. Erasmus and J. Comins, *Journal of colloid and interface science*, 309 (2007) 470.
26. H. Lgaz, A. Chaouiki, M. R. Albayati, R. Salghi, Y. El Aoufir, I. H. Ali, M. I. Khan, S. K. Mohamed, I-M. Chung, *Research on Chemical Intermediates*, 45 (2019) 2269.
27. A. Chaouiki, H. Lgaz, I-M. Chung, I. H. Ali, S. L. Gaonkar, K. S. Bhat, R. Salghi, H. Oudda, M. I. Khan, *J. Mol. Liq.*, 266 (2018) 603.
28. M. H.A. Suleiman, I. H. Ali, *Int. J. Electrochem. Sci.*, 13 (2018) 3910.
29. P. M. Richardson, *Brittonia*, 42 (1990) 115.
30. K. Wolfe, X. Wu and R. H. Liu, *Journal of agricultural and food chemistry*, 51 (2003) 609.
31. L. Yu, S. Haley, J. Perret, M. Harris, J. Wilson and M. Qian, *Journal of Agricultural and Food Chemistry*, 50 (2002) 1619.
32. A. Ordonez, J. Gomez and M. Vattuone, *Food chemistry*, 97 (2006) 452.
33. T. Osawa, *Post harvest biochemistry of plant food-materials in the tropics. Japan Scientific Societies Press, Japan*, (1994) 241.
34. J. Scully and R. Baboian, *ASTM, Philadelphia, PA*, (1995) 110.
35. Z. Salarvand, M. Amirnasr, M. Talebian, K. Raeissi and S. Meghdadi, *Corros. Sci.*, 114 (2017) 133.
36. A. Biswas, P. Mourya, D. Mondal, S. Pal and G. Udayabhanu, *J. Mol. Liq.*, 251 (2018) 470.
37. A. Dutta, S. K. Saha, U. Adhikari, P. Banerjee and D. Sukul, *Corros. Sci.*, 123 (2017) 256.
38. S. Martinez and M. Metikoš-Huković, *Journal of Applied Electrochemistry* 33 (2003) 1137.
39. H. Shih and F. Mansfeld, *Corros. Sci.*, 29 (1989) 1235.

40. F. Bentiss, M. Traisnel and M. Lagrenee, *Corros. sci.*, 42 (2000) 127.
41. S. Muralidharan, K. Phani, S. Pitchumani, S. Ravichandran and S. Iyer, *J. Electrochem. Soc.*, 142 (1995) 1478.
42. K. Alaneme, S. Olusegun and A. Alo, *Alexandria Engineering Journal*, 55 (2016) 1069.
43. S. Kumar, *Protection of Metals and Physical Chemistry of Surfaces*, 52 (2016) 376.
44. D. M. Gurudatt and K. N. Mohana, *Industrial & Engineering Chemistry Research*, 53 (2014) 2092.
45. P. Singh, E. E. Ebenso, L. O. Olasunkanmi, I. Obot and M. Quraishi, *The Journal of Physical Chemistry C*, 120 (2016) 3408.
46. M. Yadav, S. Kumar, R. Sinha, I. Bahadur and E. Ebenso, *J. Mol. Liq.*, 211 (2015) 135.
47. A. Chaouiki, H. Lgaz, S. Zehra, R. Salghi, IM. Chung, Y. El Aoufir, K. S Bhat, I. H. Ali, S. L. Gaonkar, M. I. Khan and H. Oudda, *Journal of Adhesion Science and Technology*, /doi.org/10.1080/01694243.2018.1554764.
48. L. Bammou, M. Belkhaouda, R. Salghi, O. Benali, A. Zarrouk, H. Zarrok and B. Hammouti, *Journal of the Association of Arab Universities for Basic and Applied Sciences*, 16 (2014) 83.
49. K. M. Emran, *Int. J. Electrochem. Sci.*, 9 (2014) 4217.
50. I. H. Ali and Y. Sulfab, *Transition Met. Chem.*, 38 (2013) 79.
51. I. H. Ali and Y. Sulfab, *International Journal of Chemical Kinetics*, 43 (2011) 563.
52. X. Li, S. Deng, H. Fu and G. Mu, *Corros. Sci.*, 50 (2008) 2635.

© 2019 The Authors. Published by ESG (www.electrochemsci.org). This article is an open access article distributed under the terms and conditions of the Creative Commons Attribution license (<http://creativecommons.org/licenses/by/4.0/>).